

Multi-domain fragmentation and walls' globules in a 2D lattice of charged particles with applications to pump- and pulse induced hidden states in $1T - \text{TaS}_2$.

Petr Karpov¹ and Serguei Brazovskii^{1,2,3}

¹*National University of Science and Technology "MISI", Moscow, Russia*

²*CNRS UMR 8626 LPTMS, University of Paris-Sud, University of Paris-Saclay, Orsay, France*

³*Jozef Stefan Institute, Jamova 39, SI-1000 Ljubljana, Slovenia*

(Dated: September 6, 2017)

Recent experiments on the optical pumping and the STM injection of carriers in a layered $1T - \text{TaS}_2$ have revealed an intriguing formation of patterns with networks and local globules of domain walls. The effect is thought to be responsible for the metallisation transition in this Mott insulator and for stabilization of a "hidden" state. In response to these challenges, we performed Monte Carlo simulations for the ground state, the phase transition and evolution of a classical lattice gas with a repulsive Coulomb interaction among the particles. The external pulse is simulated by introducing a small random concentration of voids into the superlattice of polarons ubiquitous to the $1T - \text{TaS}_2$. Despite the Coulomb repulsion, the single-void states are unstable with respect to their binding and progressive aggregation. With augmenting concentration of charged voids, we observe their gradual coalescence into interconnected globules of domain walls. This coalescence of voids can be understood by fractionalization of their charges within the wall separating domains with different degenerate ground states.

INTRODUCTION

The rich phase diagram of $1T - \text{TaS}_2$ includes such states as incommensurate, nearly commensurate, and commensurate charge density waves (CDW) which unusually support also the Mott insulator state for a subset of electrons. Recently, new metastable phases have been discovered: a "hidden" state created by laser [1, 2] or voltage [3] pulses, and a probably related "metallic mosaic" state created locally by STM pulses [4, 5]. This work is motivated by latest STM experiments [2–6] on visualization, manipulation and tracing the evolution of networks and globules of domain walls separating the degenerate phases of CDWs.

$1T - \text{TaS}_2$ is a narrow-gap insulator formed from a parent metal (with 1 electron per Ta site) by a high- T ($T_c > 500\text{K}$) CDW [7]. Incomplete nesting leaves each 13-th electron ungaped which in a typical CDWs would give rise to a pocket of carriers. Here, each excess carrier is self-trapped by inwards displacements of the surrounding atomic hexagon (forming the "David star" unit) which gives rise to the intragap local level accommodating this electron. These charged heavy polarons inevitably arrange themselves into the Wigner crystal. Exciting the self-trapped electron from the intragap level deprives the deformations from reasons of existence, the David star levels out in favor of a void in the crystal of polarons. A major question arises: why and how the repulsive voids aggregate into the net of walls leaving micro-crystalline domains in-between?

In this paper, we answer this and related questions by modeling the superlattice of polarons upon the 2D triangular basic lattice of all Ta atoms by a classical charged lattice gas with a screened repulsive Coulomb interaction among the particles. Here one particle represents

a polaron which is seen in $1T - \text{TaS}_2$ as a David star consisting of 13 electrons and the associated lattice distortion. The external pulse injecting the voids is simulated by introducing a small random concentration of voids reducing the particles concentration ν below the equilibrium $\nu_0 = 1/13$. The subsequent evolution of the system is studied by means of the Monte Carlo simulation. Surprisingly, this minimalistic classical model is already able to capture the experimentally observed formation of domain walls and to explain it in a natural way.

THE MODEL

We model the system of polarons by a lattice gas of charged particles on a triangular lattice. Each particle represents the self-trapped electron in the middle of the David star, thus the effective charge is $-e$, which is compensated by the static uniform positive background.

The external pulse is simulated by a small concentration of randomly seeded voids reducing the particles concentration below the equilibrium: $\nu = \nu_0 - \delta\nu$. The interaction of polarons located at sites i, j is described by an effective Hamiltonian with repulsive interactions U_{ij} :

$$H = \sum_{i,j} U_{ij} n_i n_j, \quad (1)$$

Here the sum is over all pairs of sites $i \neq j$; $n_i = 1$ (or 0) when particle is present (absent) at the site i , and we choose U_{ij} in the form of a screened Coulomb potential

$$U_{ij} = e^2 \frac{\exp(-r/l_s)}{|\mathbf{r}_i - \mathbf{r}_j|} \equiv U_0 \frac{a \exp(-\frac{r-a}{l_s})}{|\mathbf{r}_i - \mathbf{r}_j|}, \quad (2)$$

where $U_0 = e^2 \exp(-a/l_s)/a$ is the Coulomb energy of interaction of particles at neighboring sites in the Wigner crystal state with the distance $a = \sqrt{13}b$ between them (b is the lattice spacing of the underlying triangular lattice; (Fig. 1(a)), l_s is the screening length. We keep in mind also the background uniform neutralizing positive charge.

SUPERLATTICE AND ITS CHARGED DEFECTS.

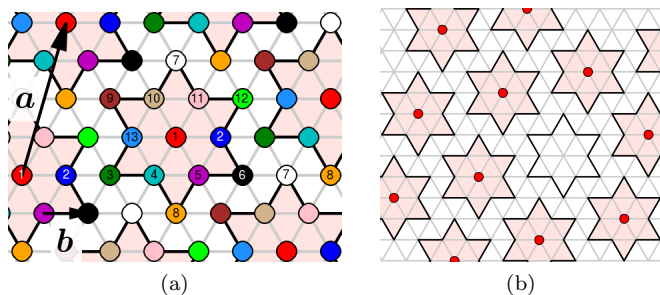


FIG. 1. (a) Lattice of Ta-atoms and the coloring scheme, showing its 13 sublattices; in the ground state only one sublattice is occupied; a is the superlattice period, b is the underlying lattice period. (b) Lattice with $\nu = 1/13$ concentration of polarons at presence of one void (the emptied “David star”). The occupied sites, marked by red circles, are surrounded by filled “David stars” which perimeters pass through neighbors which positions are actually displaced inwards.

In the ground state, all particles living on the triangular lattice tempt to arrange themselves in also the triangular superlattice, which is the close-packed and most energetically favorable in 2D [8] (with some notable exceptions for more exotic potentials [9]). Since the concentration of the particles is $1/13$, then the ground state is 13-fold degenerate with respect to translations (Fig. 1(a)); an additional mirror symmetry makes the ground state in total 26-fold degenerate. But since within a given sample two mirror-symmetric phases do not coexist both in the experiment [10] and in the modeling for the sufficiently slow cooling rates (because of the high energy of the corresponding twinning wall), then we consider only one of them.

The simplest lattice defect is a void or a “polaronic hole” (Fig. 1(b)) which is formed when the electron from the intragap level is excited to the conduction band and soon the associated lattice distortions vanish. The single void has the relative charge $+e$ (keeping in mind the background neutralizing charge) and the Coulomb self-energy of the order

$$E_{void} \simeq \frac{e^2}{a}. \quad (3)$$

While the void is a particular manifestation of a general notion of vacancies in crystals, in our case there can be

also a specific topologically nontrivial defect – the domain wall – owing to the 13-fold positional degeneracy of the ground state. If different parts of the system are in different ground states, then inevitably there should be a domain wall between them (Fig. 2). The domain wall cross-section resembles the discommensuration known in CDW systems [11].

Experimentally, the lattice defects can be introduced via external pulses, by impurity doping or by the field effect. For example, a laser or STM pulse can excite the Mott-band electrons residing in the centers of the David star clusters, creating an ensemble of voids. Since the voids are charged objects, then at first sight they should repel each other and form a Wigner crystal themselves. But our modeling consistent with the experiment shows that the voids rather attract one another at short distances and their dilute ensemble is unstable towards formation of domain wall net. Qualitatively, this instability can be understood from the following argument. Compare energies of the isolated void and of the domain wall segment carrying the same charge. The minimal charge of domain wall per the translation vector \mathbf{a}_1 is $+e/13$ (Fig. 2(a)), and the energy of the wall’s segment carrying the charge $+e$ can be estimated as for a uniformly charged line:

$$E_{wall} \simeq 13 \times \frac{(e/13)^2}{a} \ln(l_s/a), \quad (4)$$

which, for moderate screening lengths l_s , is lower than the voids’ self-energy 3, making them energetically favorable to decompose into fractionally-charged domain walls. The local effects beyond our model can also favor domain walls with other charges: for $+1e/13$ domain wall there are anomalous sites where David stars intersect (Fig. 2(a)), which raises its energy and can make $+2e/13$ domain walls more energetically favorable (Fig. 2(b)).

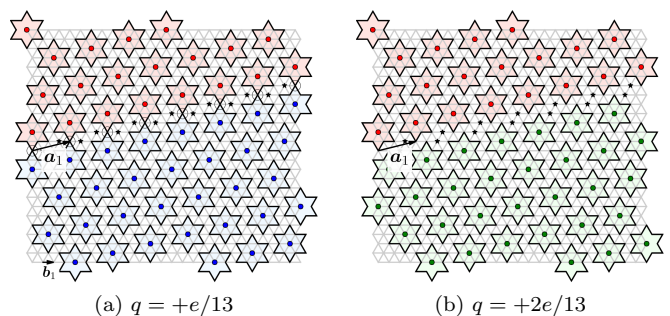


FIG. 2. Positively charged domain walls with charges per unit cell length \mathbf{a} : (a) $+e/13$; (b) $+2e/13$. The whole sequence of domain walls can be obtained by consecutive shiftings of the blue domain by the vector \mathbf{b}_1 as indicated in (a). In (a), the sites are encircled where David stars within the wall share the corners. Black asterisks show the sites not belonging to any star.

NUMERICAL MODELING

Neutral system.

We simulate the classical lattice gas with the Hamiltonian (1) and the interaction potential (2) via Metropolis Monte Carlo method. We use the screening parameter $l_s = 4.5b \approx 1.25a$ and also truncate the interactions to zero for sufficiently large interparticle distances (outside the hexagon with the side $24b$). Periodic boundary conditions are imposed.

As a reference system we chose the sample with 91×104 sites with the total a number of electrons $N_{el} = 728$ which corresponds to the concentration $\nu_0 = 1/13$. The ground state is reached after typically 7 millions of Monte Carlo steps at each temperature (which corresponds to ≈ 9600 sweeps), gradually lowering it from $T = 0.065U_0$ down to $T = 0.015U_0$ with a step $\Delta T = -0.0002U_0$. The ground state acquires the form of the triangular Wigner crystal lattice.

At $T_c \approx 0.055U_0$ we observe an order-disorder phase transition below which the triangular superlattice is formed confirming the expectations for the Wigner crystal. The temperature dependencies of the order parameter $M = \sqrt{\sum (m_i - 1/13)^2 / 13 \cdot 12}$, where m_i is the fraction of particles at i -th sublattice (Fig. 3(a)) and of the mean value of energy per particle (Fig. 3(b)) indicate that the transition is of the first order. The insets in the Fig. 3(a) show a plenty of defects just above T_c , while only two displaced positions are left just below T_c . Interestingly, for greater screening lengths we observe that the system freezes in a glass state, which is known to exist in frustrated Coulomb system without any frozen disorder [12], however for our model no frustration is necessary.

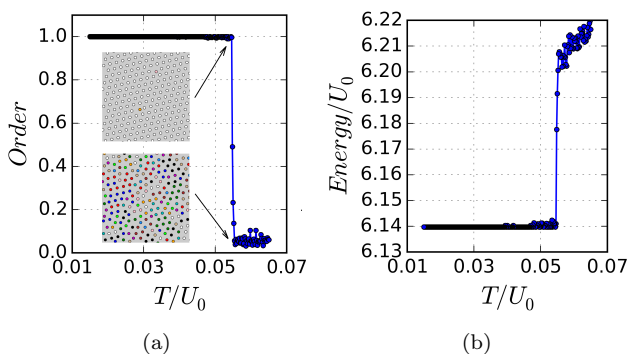


FIG. 3. Temperature dependencies of integrated characteristics for the neutral system: (a) the order parameter (blue circles); the insets show snapshots of configurations of the system just above and below the phase transition; (b) mean energy per particle.

Doped system.

We emulate the doping by seeding voids in the system at random places and following the evolution. Because of the doping, the order-disorder transition temperature slightly lowers, but more importantly a new ground state with the net of domain walls is formed as we will show below. An analogous phase transition to the charged domain walls' ground state induced by pump of field doping is predicted for quasi-1D polyacetylene-like systems with 2-fold degeneracy [13].

Seeding at $T < T_c$ a small number of voids, down to two voids in the sample, we observe that the single-void states are unstable with respect to their binding and progressive aggregation. Seeding more voids initiates their gradual coalescence into a globule of interconnected segments of domain walls. The resulting globule performs slowly a random diffusion over the sample while keeping closely its optimal shape and the structure of connections.

Figure 4(a) shows a low T state after 8 voids have been introduced and the system was cooled from $T = 0.065U_0 > T_c$ down to $T = 0.015U_0$. In spite of the initial random distribution of particles over the whole sample, finally the voids aggregate into a single globule immersed into an infinite connected volume of the unperturbed crystal. We compare the results of our modeling in Fig. 4(a) with the experimental picture in Fig. 4(b) [4] (note that similar patterns have been observed also in other experiments: [3]-Fig. 3 of the supplement and [5]-Fig. 1). With a further increase of doping, the globule size grows, becoming comparable to the sample size, and the branched net of domain walls divides the system in similar-sized domains of random shapes (Fig. 5(a),(c)), which we compare with (similar patterns for optical switching can be found [2]).

We notice a spectacular resemblance of our modeling with results from several STM experiments. The results for the high doping correlate with the STM pictures obtained after the current injection [4, 5] or the optical pumping [2]. The comparison of the modeling with the experiment on injection by the STM pulses is shown between panels (a) and (b) in Fig. 4, between panels (a) and (b), (c) and (d) in Fig. 5.

DISCUSSION AND CONCLUSIONS

Our numerical simulations show an apparently surprising behavior: some effective attraction of defects develops from the purely repulsive Coulomb interactions. Even for a small voids' concentration, single-voids are unstable with respect to their aggregation. For several voids seeded, we observe a gradual fusion of point defects into the net of the domain walls. Increasingly branched net develops with augmenting of the voids concentration.

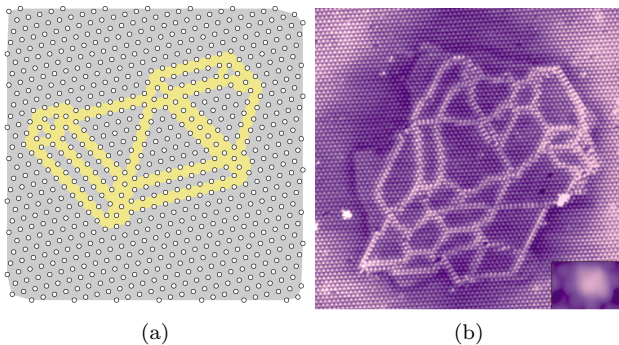
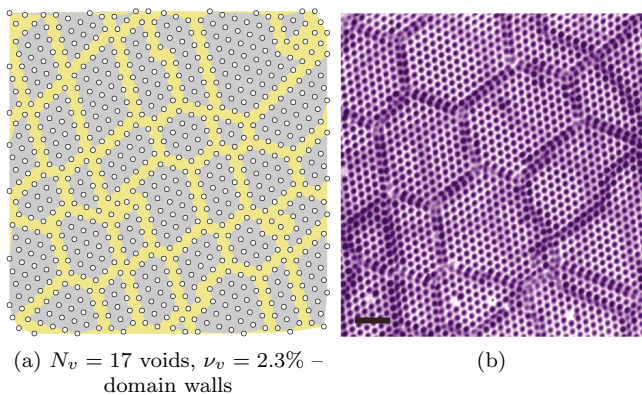
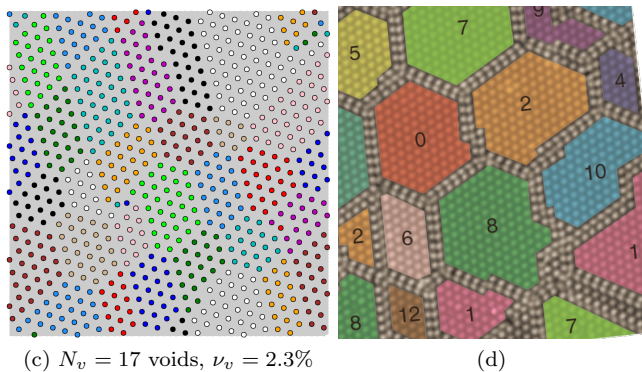


FIG. 4. Globule structures. (a) The present modeling: $N_v = 8$ voids, $\nu_v = 1.1\%$ in the domain walls representation; (b) from experiments in [4].



(a) $N_v = 17$ voids, $\nu_v = 2.3\%$ – domain walls



(c) $N_v = 17$ voids, $\nu_v = 2.3\%$

(d)

FIG. 5. The modeling for a high doping (a,c) vs experiments (b,d). Maps of domain walls (a,b) and of domains (c,d). Figs. (a,c) show the present modeling with $N_v = 17$ voids at $T = 0.015U_0$, the coloring scheme for domains is indicated in Fig. 1. Figs. (b,d) are adapted from [4], numbers in Fig. (d) show the corresponding coloring scheme for domains.

That can be understood indeed by noticing that the walls formation is not just gluing of voids but their frac-

tionalization. The domain wall is fractionally ($q = \nu_0 e$) charged per its crystal-unit length, thus reducing the Coulomb self-energy in comparison with the integer-charged single void. Being the charged objects, the domain walls repel each other but as topological objects they can terminate only at branching points, thus forming in-plane globules. Their repulsion at adjacent layers meets no constraints, hence the experimentally observed alternation of the walls' patterns among the neighboring layers [2, 4, 5].

The proposed minimalistic statistical model already captures many interesting effects, but not all of them. We did not consider the case of doping by electrons – here the interstitial David stars substantially overlap with their neighbors giving rise to stronger lattice deformations, which require a more complicated model.

Still the encouraging visual correspondence of our pictures with experimentally obtained patterns – for different regimes of low and high levels of doping – ensures a dominant role of the universal model.

The authors are grateful to D. Mihailovich, Y.A. Gerasimenko, and H.W. Yeom for helpful discussions. We acknowledge the financial support of the Ministry of Education and Science of the Russian Federation in the framework of Increase Competitiveness Program of NUST MISiS (No. K3-2017-033). SB acknowledges funding from the ERC AdG “Trajectory”. Image source for Fig. 4(b), 5(b),(d): [4]; use permitted under the Creative Commons Attribution License CC BY 4.0.

-
- [1] L. Stojchevska, I. Vaskivskiy, T. Mertelj, P. Kusar, D. Svetin, S. Brazovskii, D. Mihailovic, *Science* **344**, 177 (2014).
 - [2] Y.A. Gerasimenko, I. Vaskivskiy, and D. Mihailovic, arXiv:1704.08149 (2017).
 - [3] I. Vaskivskiy, et al., *Nature Comm.*, **7**, 11442 (2016).
 - [4] L. Ma et. al., *Nature Comm.* **7**, 10956 (2016).
 - [5] D. Cho et. al., *Nature Comm.* **7**, 10453 (2016).
 - [6] D. Cho et. al., arXiv:1706.08607 (2017).
 - [7] K. Rossnagel, *J. Phys. Condens. Matter* **23**, 213001 (2014).
 - [8] L. Bonsall and A. A. Maradudin, *Phys. Rev. B* **15**, 1959 (1977).
 - [9] E. A. Jagla, *Journ. Chem. Phys.* **110**, 451 (1999).
 - [10] H. Shiba and K. Nakanishi in “Structural Phase Transitions in Layered Transition Metal Compounds”, ed. K. Motizuki (D. Reidel Publishing Company, Dordrecht, 1986).
 - [11] W.L. McMillan, *Phys. Rev. B* **14**, 1496 (1976).
 - [12] S. Mahmoodian, L. Rademaker, A. Ralko, S. Fratini, and V. Dobrosavljevic, *Phys. Rev. Lett.* **115**, 025701 (2015).
 - [13] P. Karpov, S. Brazovskii, *Phys. Rev. B* **94**, 125108 (2016).